Microstructural characterization of a composite Mo reinforced by 25 at.% TiC

D. Cédat [a], C. Rey [a,*], M. Clavel [a], J.H. Schmitt [a], M. Le Flem [b], A. Allemand [c]

[a] Laboratoire de Mécanique des Sols, Structures et Matériaux, UMR 8579, Ecole Centrale Paris, Grande Voie des Vignes, 92295 Châtenay-Malabry cedex, France
[b] DEN/DANS/DMN/SRMA/LA2M, CEA, Centre de Saclay, 91191 Gif-sur-Yvette, France
[c] DEN/DANS/DMN/SRMA/LTMEX, CEA, Centre de Saclay, 91191 Gif-sur-Yvette, France

ABSTRACT

In the scope of cermet development for structural pieces of future nuclear reactors (1000–1650 °C), Mo–$TiC_{25at.\%}$ was processed by hot isostatic pressure (HIP) and characterized in term of microstructure and chemical composition. The fabrication resulted in a three-phase material so called core/shell microstructure. Scanning electron microscopy (SEM) and transmission electron microscopy (TEM) analyses, both coupled with X-ray detection (EDX), allowed to highlight the formation of TiC–$Mo_{15at.\%}$ phase at the TiC/Mo interface, in agreement with the phase diagram. The formation mechanisms of this phase are discussed.

© 2009 Elsevier B.V. All rights reserved.

1. Introduction

Titanium carbide (TiC) matrix composites were widely studied in 1980s [1] and some reviews on the modern cermets are given in the literature [2–5]. Because of their high hardness, thermal stability, relatively high thermal and electrical conductivities, as well as excellent creep and wear resistance, those cermets have been successfully used for cutting tools in finishing work of steel and iron.

The major constituents of the composite studied in this paper consist of fine molybdenum particles, which are soft and ductile, and the minor constituent of titanium carbide which is hard and brittle. In fact, the use of these Mo–TiC composites is developed within the framework of the refractory materials' applications for the core lay-out structure in gas cooled reactor (GCR). Indeed, the requirement for high-performance structural materials that can offer attractive combinations of high specific strength and stiffness, efficiency and reliability, over wide range of operating temperatures, has catalysed considerable scientific and technological interest in the development and use of hybrid materials or composites. Nevertheless, both hard and metal phases are, to some extent, modified by refractory carbides and respectively, in order to achieve certain targeted properties. Thus, the materials science of such compound must include the scientific knowledges related to both ceramic and metal phases. The fundamental reason for characterising these microstructures is to provide a base for understanding their mechanical and physical properties for the purpose of developing more effective nuclear materials.

The investigated material ($MoTiC_{25at.\%}$) has been processed by hot isostatic pressure (HIP) at 1600 °C what it makes the difference compare to most of industrial cermets which are forming by liquid phase sintering [6].

This work focuses on a microstructural characterization of this new elaborated material and, in particular, on the formation of a third phase existing between the core and the matrix.

2. Experimental

2.1. Samples preparation

Both titanium carbide ($d_{50} = 3 \mu m$) and molybdenum ($d_{50} = 5 \mu m$) were supplied by HC Starck. TiC and Mo chemical analysis is given in Table 1.

The composite powder is obtained by milling of TiC and Mo in alcohol during two hours, with zirconia balls. After alcohol evaporation, the mixing powder is introduced in a latex can and shaped by cold isostatic pressing at 2500 bar during 1 min. After this step, the green sample is placed in a titanium can and an out gassing in high-vacuum at 600 °C during 12 h was carried out. The sintering step is produced by hot isostatic pressing at 1600 °C during 2 h under a pressure of 1610 bar. The density obtained is $d = 8.52$ with a total porosity of 1.24% (isolated porosity = 1.13%).

2.2. Experimental procedure

Scanning electron microscope (SEM) coupled with electron back scatter diffraction (EBSD) was carried out in order to characterise the microstructure and the orientation of each grain. The post-processing, using image analyses, of the picture obtained by SEM, allows to quantify the proportions of the three phases constituting

* Corresponding author. Tel.: +33 (0) 141 13 15 73; fax: +33 (0) 141 13 14 30.
E-mail address: colette.rey@ecp.fr (C. Rey).

Table 1
Table of composition of commercial TiC and Mo composition.

C_{total}	O	N	Ca	Co	W	Ni	Al	Fe	S
TiC composition (wt%)									
19.23	0.6126	0.0279	0.002	0.032	0.39	<4E−4	0.0014	0.0061	0.0019
Mo		O				Fe			K
Mo composition (wt%)									
99.8		0.0620				9 ppm			29 ppm

the material. Moreover the composition of these phases has been investigated by X-ray analyses using energy dispersive X-ray method (EDX), thanks to a Philips Teknai F20 (200 kV). A thin foil of composite was used, so as to the X-rays were confined to a region close to primary beam and to avoid absorption and fluorescence corrections. The EDX technique was also used to analyse the compositional variation across the core/shell/binder region. In order to obtain, a more accurate composition of the phases, electron probe microanalysis (EPMA) was carried out. The use of wavelength dispersive spectrometers (WDS) allows much better peak resolution and, therefore, helps to resolve peak overlap problems.

To make the identification of each phase better, transmission electron microscopy (TEM) observations were carried out. Thus, disks of 3 mm diameter and 2 mm in thickness were cut from the rod before any deformation, in a plane perpendicular to the rod axis. The TEM foils were prepared by the method of ion beam etching. The microstructure was examined by transmission electron microscopy (TEM) using a JEOL JEM 1200 EX, 120 kV.

2.3. Samples characterization

The microstructure of the sintered TiC/Mo composite (Mo–TiC 25at.%) can be seen in Fig. 1 which shows a scanning electron micrograph. This micrograph was obtained using backscattered electrons. It can be seen that there are both bright and dark cores, surrounded by grey rim. The bright cores contain heavier atoms, in this case Mo (BCC structure), and the darker are TiC (FCC structure). The grey phase will be named (Mo,Ti)C phase in all the continuation of this paper. Thus, the hard particles (TiC) can be seen to have what is referred to as a core/shell or core/rim structure with molybdenum as binder phase. Fig. 2 shows that the (Mo,Ti)C and the TiC phases cannot be differentiated and are composed of small (1–2 μm) misoriented grains. Molybdenum grains are about 2–3 μm. No texture was observed after the process.

Concentration profiles of Ti and Mo were measured through line analysis across a coarse TiC grain (Fig. 3), obtained on a secondary electron image of the composite. The concentration of molybdenum gradually decreases from the highest level in the binder phase to the lowest value in the core, whereas the concentration of titanium decreases from the core to zero in the binder phase. A composition plateau is also observed in the middle of surrounding layer and no diffusion profile was observed what it allows us to assume that the surrounding layer has a definite composition.

Although the experimental evidence is strong for a sharp discontinuity in composition between core and shell, the question of whether there is a composition gradient or not across the shell has to be solved.

The X-ray elemental maps of Ti, Mo in the cermet, coming from the area defined by a red[1] square, are given in Fig. 4. A sharp boundary at the core/shell interface can be pointed out. The EDX results showed that the shell regions composition were reasonably constant (Fig. 5).
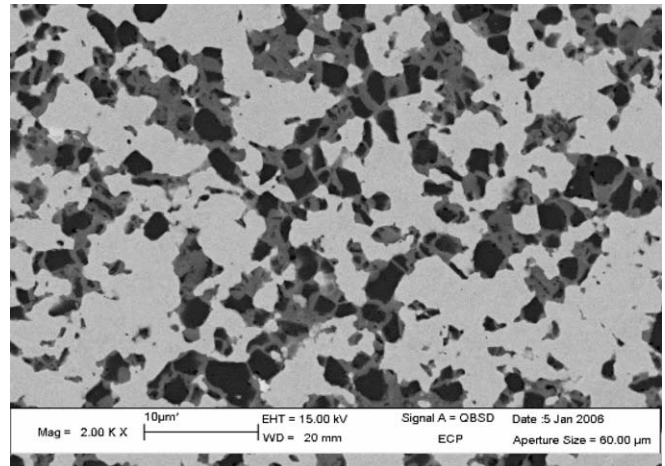
---

[1] For interpretation of color in Figs. 2–5 and 8–10, the reader is referred to the web version of this article.

Fig. 1. SEM picture showed microstructure in Mo–TiC$_{25at.\%}$.
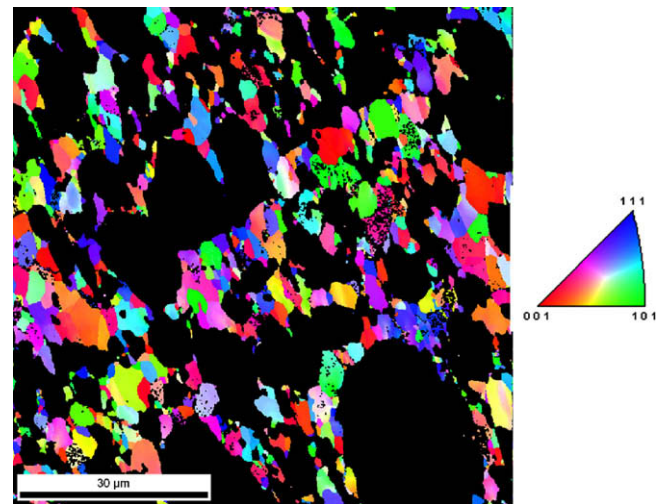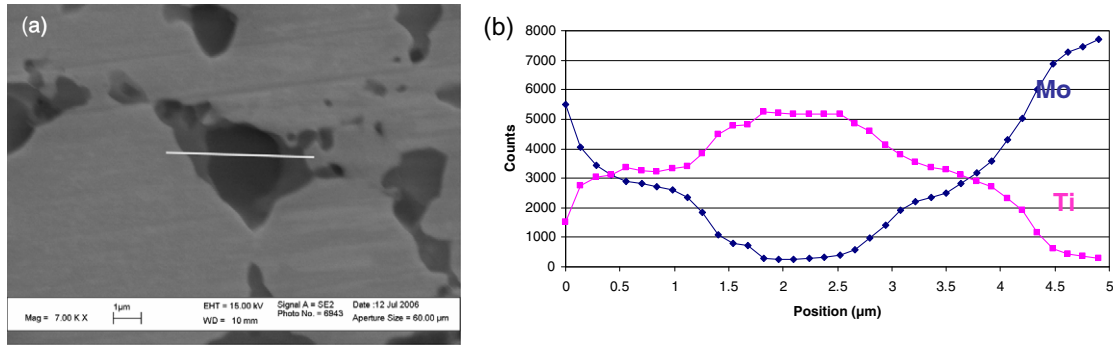

Fig. 2. Inverse pole figure map showing the position of the normal axis in the stereographic triangles for TiC (FCC).

The WDS experiments proved that (Mo,Ti)C phase exhibits a composition close to the solid solubility of molybdenum in the titanium carbide: TiC–Mo$_{10–15at.\%}$ [7]. These measures are consistent with the phase diagram of the binary system Mo–TiC (Fig. 6). As a matter of fact, the solid solubility of molybdenum in TiC could reach 25 at.% at the eutectic (MoTiC$_{35at.\%}$ at 2175 °C) and has been reported [8] at about 15 at.% in the temperature range of 1710–2000 °C with a little change in solubility at lower temperatures.

TEM observations showed that the grain size of TiC is close to 1 μm whereas the grain size of Mo is about 2–3 μm, what is in agreement with EBSD measures. To highlight the core/shell structure of the cermet, TEM observations were carried out, as shown in Fig. 7, and the shell phase (Mo,Ti)C, already observed Fig. 1, can be identified at the grain boundary between TiC and Mo grains. The presence of precipitates shows that this composite has further additional elements arising from commercial TiC powder, which add to the complexity of structural characterization. Grain boundaries between molybdenum grains are particle free. Thus, the diffusion of molybdenum into carbide phase during sintering procedure would be a possible mechanism to explain the formation of the (Mo–Ti)C phase.

Fig. 3. (a) SEM image micrograph showing the microanalysis line through core/shell structure. (b) Ti and Mo atomic concentration profile obtained by microanalysis EDX through core/shell structure.

The measured density of dislocations, in TiC is close to $\rho = 10^{12} \text{ m}^{-2}$. The dislocations with a $\langle 1 1 0 \rangle$ Burgers vector present a rearrangement, in a hexagonal configuration (Fig. 8) pointing out a recovery phenomenon and the lack of dislocation in molybdenum grains suggests that a phenomenon of recrystallisation occurred during the sintering step.

A special attention is paid to the XDR analyses (Fig. 9). In fact, the shape of each peak of TiC presents a shoulder what it means that a secondary phase presents a similar structure. The [2 2 0]

ray of TiC presents two peaks because the resolution become better at high values angles. According to the phases of the material, we could assume that the (Mo,Ti)C phase has a face centred cubic structure with a lattice parameter close to TiC.
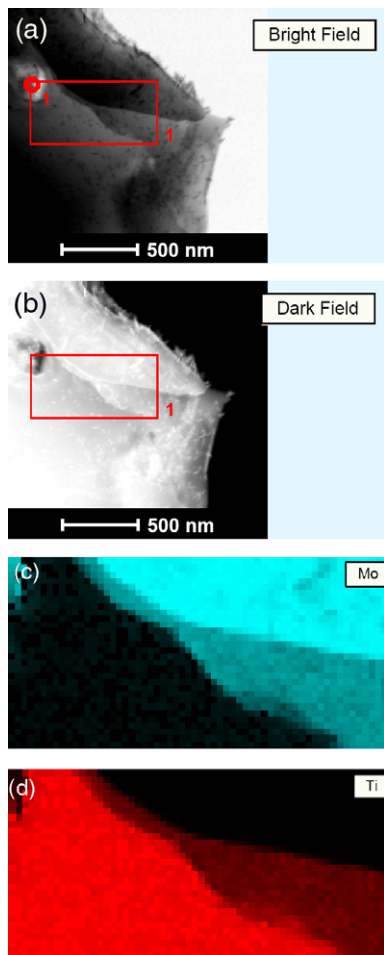
Fig. 4. Energy dispersive X-ray element maps acquired by STEM. (a) Picture of thin foil of composite (TEM dark field); (b) picture of thin foil of composite (TEM bright field); (c) map of Mo element; and (d) map of Ti element.
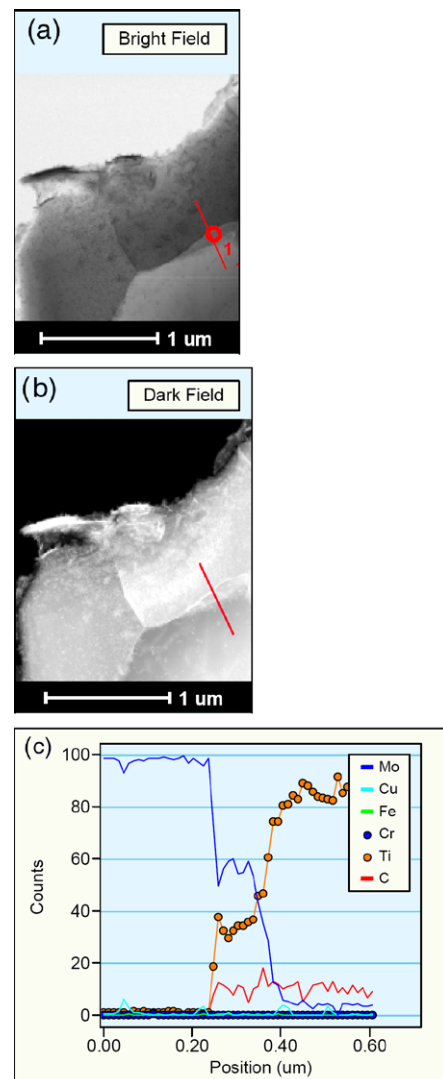
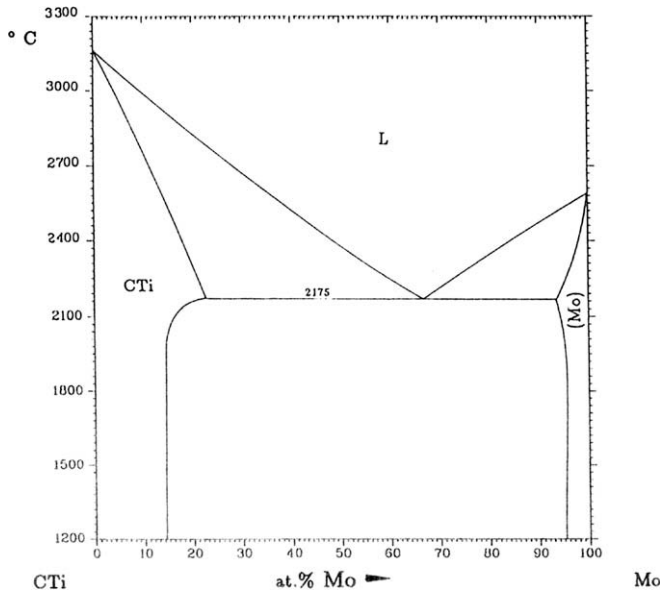**Fig. 5.** Compositional variation across the TiC/(Mo,Ti)C/Mo region from EDS measurement.

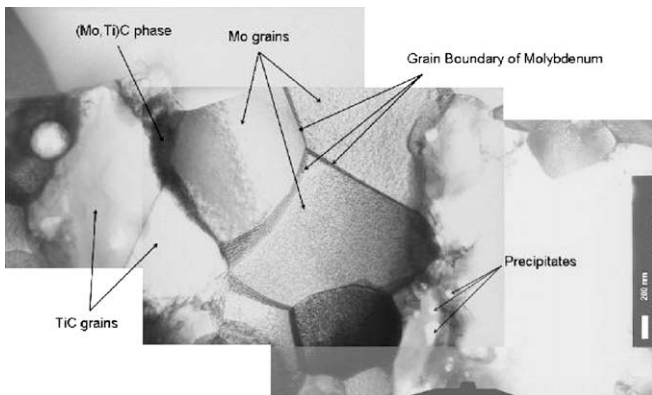**Fig. 6.** Diagram phase of ternary system Mo–Ti–C.

Fig. 7. Transmission electron micrograph picture showing core/shell structure in a Mo–TiC$_{25at.\%}$ cermet.

Fig. 8. Transmission electron micrograph showing (a) the rearrangement on hexagonal configuration and (b) density of dislocations in TiC phase.

3. Results and discussion

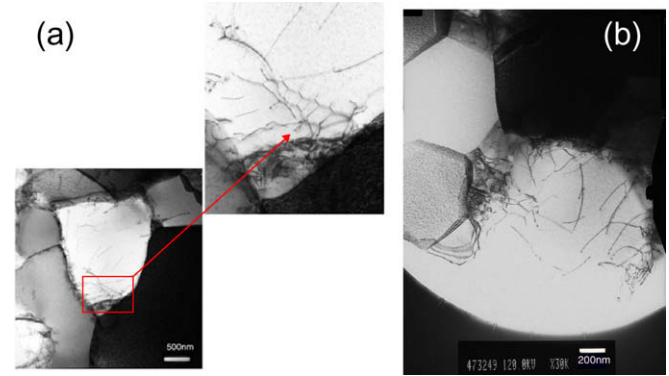Our results suggest a diffusion of molybdenum in the carbide during sintering. We assume that at the early stages of the sinter-ing cycle, the formation of the core/shell microstructure could be caused by solid state sintering and diffusion, explaining why this phenomenon occurs well below the eutectic temperature of the Mo–TiC alloy. However, it is quite apparent the TiC–Mo system has retained its thin particle size. It is also apparent that the shell film is thin and is present all around each hard particle (TiC). Our results fitted with the grain size evolution already treated in numerous publications [9] concerning the various production parameters such as initial particle size and size distribution, sinter-ing temperature and sintering periods.

The diffusion of the molybdenum in the titanium carbide can be enhanced during the sintering owing to the fact that TiC belongs to the group IV transition metal carbides.

An important property of these transition metals having the NaCl-type structure is the fact that the octahedral interstitial sites of metallic fcc sub-lattice may be only partially filled with carbon atoms, i.e. the presence of structural defects such as vacancies. Un-der certain conditions, a redistribution of non-metal atoms and structural vacancies on the interstitial lattice sites were already re-ported. Owing to their high structural vacancy concentration and rather high atomic mobility of the interstitial atoms, titanium car-bides display a far greater variety of superstructures and it was shown that several ordered carbide structures can form [10]. Con-sequently, in the early sintering stages, the matter transport in-volves essentially the diffusion process, filling thus in the necks at the points of contact between the powders particles. However, the completion of neck (concave regions) reduces the surface en-ergy and thus makes of these regions some sinks and sources of vacancies. The stress gradient and the difference in gradient in va-cancy concentration make the material transfer easier by the phe-
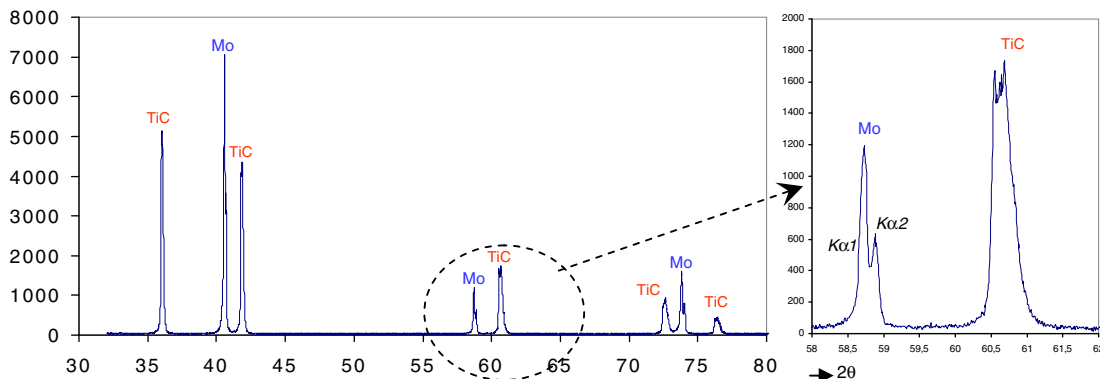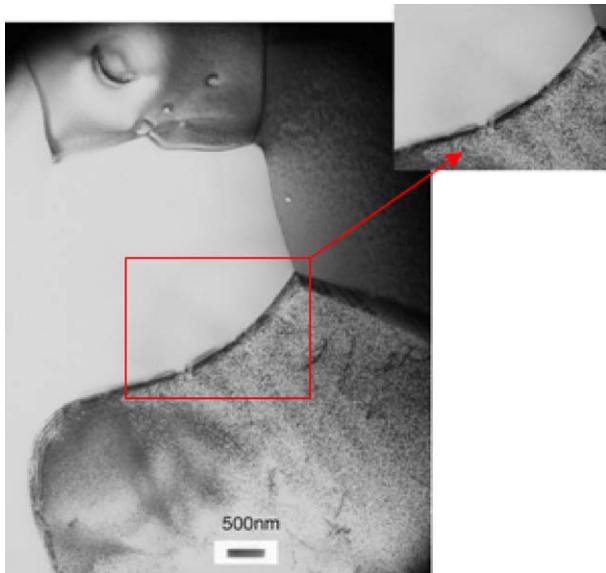

Fig. 9. XRD observation of Mo–TiC showing a double pick for the [2 2 0] ray.

Fig. 10. Local stress concentration in the interface TiC–Mo showing a relaxation of these stresses by presence of dislocations.

nomena of diffusion along the surface and grain boundaries or volume diffusion. The predominant role of grain boundaries as sinks for vacancies arriving from the neck surface was reported in literature [11].

This assumption of cermets' formation is strengthened by the lack of dislocation in molybdenum phase which can be explained by this phenomenon of recrystallisation. In fact, during the sintering step, molybdenum phase undergoes conditions such that thermal equilibrium is not any more realized. Thus, under such conditions with high dislocations density, the recrystallisation of molybdenum was possible. Indeed, the formation of this microstructure, in particular (Mo,Ti)C phase, is due to the high dislocation density which enhanced pipe diffusion of molybdenum and the partial annealing of the (Mo,Ti)C phase.

To explain the presence of dislocation in TiC grains it is necessary to remind that the compositions of the core and the binder being different, these phases have different coefficients of thermal expansion leading to differential thermal contraction when the cermets are cooled to room temperature. These results indicate that the hard phase is subjected to local stress concentrations

which are sufficient to generate dislocations in titanium carbide grains as shown in Fig. 10.

4. Conclusion

Investigation of concentration changes in the carbide solid solution by the usual methods show the least difference between core and shell for these alloys. SEM, TEM, and X-ray diffractometry investigation were required for measurement and identification of phase and phase distribution. TiC–Mo microstructures have been analysed and it has been emphasised that the outstanding characterization problem is one of quantification of TiC–$Mo_{10-15at.\%}$ phase size, and its volume fraction. Thus, it seems necessary to correlate knowledge of these parameters with mechanical cermet properties in a systematic way.

In fact, throughout this paper, we attempted to describe the involved mechanisms during the sintering of the cermet. Finally we proceeded to a fine characterization of its microstructure. Thus, that carries to believe that (Mo,Ti)C content, originating from the Mo and TiC powders, is probably caused by the diffused phases recrystallisation as the shell.

References

[1] H. Kurishita, R. Matsubara, J. Shiraishi, H. Yoshinaga, Trans. Jpn. Inst. Metals 28 (1) (1987) 20.
[2] R. Kieffer, P. Ettmayer, M. Freudhofmeier, in: H. Hausner (Ed.), Modern Development in Powder Metallurgy, vol. 5, 1971, p. 201.
[3] P. Ettmayer, W. Lengauer, Powder Metall Ont. 21 (2) (1989) 31.
[4] H. Pastor, Mater Sci. Eng. A 105/106 (1988) 401.
[5] P. Ettmayer, H. Kolaska, W. Lengauer, K. Dreyer, Int. J. Refract., Met. Hard Mater. 13 (1995) 343.
[6] P. Ettmayer, H. Kolaska, in: H. Bildstein, H.M. Ortner (Eds.), 12th Plansee Seminar'89, vol.2, p. 771.
[7] Développement de Cermets Mo–TiC pour les systèmes nucléaires du futur, Marion Le Flem, Alexandre Allemand, Stéphane Urvoy, Denis Cédat, Colette Rey, Congrés Matériaux 2006, Dijon, France.
[8] H.N. Eremenko, Handbook of ternary Alloy Phase diagrams, vol. 6, American Society for Metals, Materials Park, OH, 1995. p. 7089.
[9] J. Gurland, J. Metals 6 (1954) 285.
[10] E. Parthé, K. Yvon, Acta Cryst. B 26 (1970) 153.
[11] H. Ichinoise, G.C. Kuczynski, Acta Metall. 10 (1962) 205.